Philosophical Magazine

ISSN: 1478-6435 (Print) 1478-6443 (Online) Journal homepage: http://www.tandfonline.com/loi/tphm20

The electronic and optical properties of a triexciton in CdSe/ZnS core/shell quantum dot nanocrystals

Abdurrahman Akturk, Hatice Tas, Koray Köksal & Mehmet Sahin

To cite this article: Abdurrahman Akturk, Hatice Tas, Koray Köksal & Mehmet Sahin (2016): The electronic and optical properties of a triexciton in CdSe/ZnS core/shell quantum dot nanocrystals, Philosophical Magazine, DOI: 10.1080/14786435.2016.1143129

To link to this article: http://dx.doi.org/10.1080/14786435.2016.1143129

Published online: 25 Feb 2016.

PHILOSOPHICAL MAGAZINE, 2016
http://dx.doi.org/10.1080/14786435.2016.1143129

Taylor & Francis
Taylor & Francis Group

The electronic and optical properties of a triexciton in CdSe/ZnS core/shell quantum dot nanocrystals

Abdurrahman Akturk[a], Hatice Tas[b], Koray Köksal[c] and Mehmet Sahin[b]

[a]Faculty of Sciences, Department of Physics, Selcuk University, Konya, Turkey; [b]Faculty of Engineering, Material Science and Nanotechnology Engineering, Abdullah Gül University, Kayseri, Turkey; [c]Architecture and Engineering Faculty, Materials and Metalurgical Engineering Department, Bitlis Eren University, Bitlis, Turkey

ABSTRACT

In the study, we aim to investigate the electronic and optical properties of single excitons, biexcions and triexcitons in a CdSe/ZnS core/shell quantum dot nanocrystal. The electronic structure has been determined by solving of the Poisson–Schrödinger equations self-consistently. In calculations, the exchange-correlation effects between identical particles have been taken into account in the frame of the local density approximation. We have demonstrated that the optical properties of triexciton systems are remarkably different from the single and biexciton systems. Absorption peaks or transition energies of the triexciton system are well separated from those of single- and bi-exciton systems. We have observed that the core-radius dependent transition energy variations of triexcitons are higher when compared with single- and bi-excitonic systems. The transition energy shifts of double and triple excitons with respect to the single exciton have been calculated as a function of the core radius and we have shown that the energy shifts are inversely proportional with the radius. We have also investigated the radius-dependent changes in binding energies and lifetimes of the structures and the comparative results have been discussed in a detail manner.

ARTICLE HISTORY
Received 2 October 2015
Accepted 12 January 2016

KEYWORDS
Quantum dots; semiconductor nanocrystals; multiexciton in nanocrystals

1. Introduction

In the last two decades, the excitonic structures in the semiconductor quantum dot nanocrystals (QDNCs) have attracted a great attention and have been investigated both experimentally and theoretically by a number of authors [1–6]. The most interesting characteristics of these structures are the possibility of manipulation of some physical properties, such as energy levels, absorption and emission wavelengths, carrier lifetimes etc., by changing the size of the QDNCs. Single- and multiexciton structures in QDs are promising candidates for applications such as optics and photovoltaics because their electronic and optical properties can be relatively easily controlled. Therefore, QDNCs are still a hot-topic subject of the research areas and technological interest due to their importance in new generation hi-tech devices such as single photon light sources, LEDs [7,8], photovoltaics [9,10] and laser devices [11,12]. The application areas of QDNC are

CONTACT Mehmet Sahin mehmet.sahin@agu.edu.tr

not restricted just optoelectronics. Another application area of the QDNCs is quantum information technology. Among the heterostructures, the QDNCs have attracted great attention to be used as quantum bits which is fundamental for the quantum computation [13–17]. In addition to all of these, recently, the QDNCs have been started to use in biology and medicine. Recent studies show that QDNCs have also great potential for the imaging techniques in neuroscience [18]. The QDNCs can also be used as biosensors to detect the patogens such as *Escherichia coli* and hepatitis B [19]. In result of the fluorescence microscopy utilized illumination properties of the QDNC, the visualizations of cells and living tissues have been carried out higher resolution in proportion to lens-based microscopy techniques [20,21].

Multiexciton generation (MEG) and recombination in semiconductor QDNCs and the understanding of its fundamental physical properties are crucial especially in new generation electronic and photonics device applications. As is well known, the simplest multiexciton (MX) structure is a biexciton (XX) which contains two-electron and two-hole. As similar to an XX, a triexciton (TX) structure is formed three-electron and three-hole. It has been reported that the process of MEG in NCQDs leads to improving the photocurrent in photovoltaic applications [22]. In this context, Smith and Binks [23] have proposed the MEG as an alternative process in colloidal QDs to increase the efficiency of the solar cells. The effect of quantum confinement on the MX states such as XX and TX states in QDNCs has been studied in last two decades, but all of these studies are still in their almost early stages. In order to understand the electronic and optical properties of the MX structures in QDNCs, some studies have been performed and reported in the literature. Zohar et al. [24] studied the role of the effective mass, band mixing and phonon emission on MEG in IV–VI nanocrystals by using a 4-band $\vec{k} \cdot \vec{p}$ effective mass model. They found that MEG efficiencies are maximized when the hole effective mass is small and close to the electron effective mass. Klimov [25] has reported a review article on spectral and dynamical properties of multiexcitons in semiconductor nanocrystals. Nozik [26] has presented a comprehensive review, in which various experiments based on time-resolved femtosecond to nanosecond spectroscopy and theoretical models for explaining the MEG in semiconductor QDs has been investigated. As a matter of fact, most of the studies related to MX or MEG are especially about XX structures rather than TX ones.

For the first time, Ikezawa et al. [27] have observed a triexciton state in quantum dots under high-density or two-colour excitation condition. Caruge et al. [28] have reported the power dependence of the TX, XX and single X emission intensities. In their study, they have demonstrated that the MX bands appeared on the blue side of the band edge emission peak stemmed from a TX recombination. Oron et al. [29] have presented a method to perform multiexciton spectroscopy in colloidal semiconductor nanocrystals via quasi-continuous-wave optical pumping. The experiments show that the emission spectra of a quantum system including TX can be easily distinguished from single X or XX systems [20,30] because a TX emission exhibits blue shift while single X or XX has red one. In addition, the fluorescence peak of TX is sharper than those of single X and XX structures [20].

The pioneering studies about the theoretical investigation of TX system in a single QD started in 1990s [31–33]. First theoretical study on tri- and quad-excitons has been revealed by Barenco and Dupert [31]. In this study, they have calculated the energy levels of multiple excitons in a quantum box and also they have computed the electron–hole, electron–

electron and hole–hole interactions [31]. Later, Hawrylak obtained energy eigenvalues by adding the effect of Coulomb and exchange interactions between the carriers for the parabolic quantum dot systems which include less than six excitons [34]. Franceschetti and Troparevsky [35] have theoretically investigated the radiative recombination of the TXs in colloidal QDNCs. Also they have shown that temperature dependence of the $p-p$ emission band resulted from the dark–bright splitting of the TX ground state.

The main objective of our study is to enlighten theoretically to the electronic and optical properties of the single X, XX and TX structures in a CdSe/ZnS core/shell QDNC. In this context, we have comparatively investigated transition, total and binding energies, overlap integrals and lifetimes of the structures as a function of the core radius in a large interval. The results have been given as a function of the core radius and their probable physical reasons have been discussed in a detailed manner.

2. Model and theory

In the study, the structure of the QD is considered as a core–shell nanocrystal. The radial potential profile and schematic diagram of this structure can be seen in Figure 1. This structure is manufactured by growing ZnS shell material which has the wider band gap on CdSe which is the core material. Nowadays, II–VI core–shell nanocrystals such as CdSe/CdS, CdSe/ZnS etc. can be synthesized in high quality [36–38]. The required parameters used in this study are taken from the previous study of Sahin et al. [6]. As is well-known, solving of a TX Schrödinger equation is very complex because of 15 Coulomb interactions between carriers as well as 6 kinetic energy terms. Therefore, it is indispensable to make some approximations and simplifications. For this purpose, the

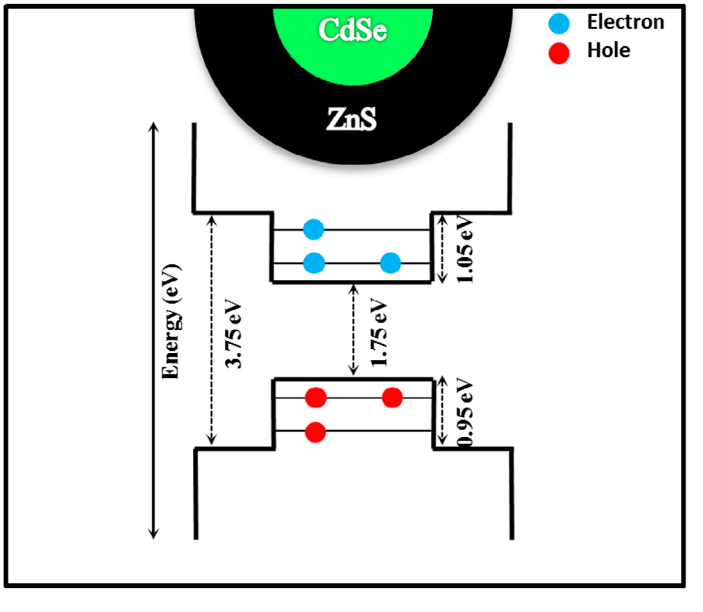

Figure 1. (colour online) A schematic representation and potential profile of the CdSe/ZnS core/shell QDNC. The confinement potential for the electrons and holes are, respectively, $V_e = 1.05$ eV and $V_h = 0.95$ eV.

Poisson–Schrödinger equations are solved self-consistently in the Hartree approximation. A single exciton radial Schrödinger equation in a TX structure reads

$$\left[-\frac{\hbar^2}{2}\vec{\nabla}_e\left(\frac{1}{m_e^*(r_e)}\vec{\nabla}_e\right)-\frac{\hbar^2}{2}\vec{\nabla}_h\left(\frac{1}{m_h^*(r_h)}\vec{\nabla}_h\right)+\frac{\ell(\ell+1)\hbar^2}{2m_e^*(r_e)r_e^2}+\frac{\ell(\ell+1)\hbar^2}{2m_h^*(r_h)r_h^2}+V_{eff}^e+V_{eff}^h\right]\psi_i(\vec{r}_e,\vec{r}_h) = E_i\psi_i(\vec{r}_e,\vec{r}_h) \quad (1)$$

where $\hbar$ is reduced Planck constant, $m_{e,h}^*$ is effective mass of electron/hole, ℓ is the orbital quantum number. First two terms indicate the kinetic energies for electron and hole, respectively. Third and fourth terms are angular momentum contribution of electron and hole in the TX system. $V_{eff}^{e,h}$ is the effective potential for electrons/holes and includes confinement, Coulomb and exchange-correlation (XC) potentials. It is noted that the XC potential between electrons and holes is not considered since its contribution is too small, approximately order of 10^{-4} meV [5]. $\psi_i(\vec{r}_e,\vec{r}_h)$ shows the wave function and E_i represents the energy levels of TX system. The exact analytical solution of this equation is still impossible and the direct numerical solution is also not so simple and therefore, more approximations are required. In a single exciton structure, the electron moves in an average potential formed by the holes and similarly the hole moves in an average potential formed by the electrons. In this case, Schrödinger equations of the electron and hole can be separately written as [39]

$$\left[-\frac{\hbar^2}{2}\vec{\nabla}_e\left(\frac{1}{m_e^*(r)}\right)\vec{\nabla}_e-q_e\phi_h+V_e(r)\right]R_e(r)=\varepsilon_e R_e(r), \quad (2)$$

$$\left[-\frac{\hbar^2}{2}\vec{\nabla}_h\left(\frac{1}{m_h^*(r)}\right)\vec{\nabla}_h-q_h\phi_e+V_h(r)\right]R_h(r)=\varepsilon_h R_h(r). \quad (3)$$

In these equations, $q_{e,h}$ and $R_{e,h}(r)$ are the charge and radial wave function of the electron and hole, respectively. $\phi_{e,h}$ is the electrostatic potential originated from electrons/holes.

In order to determine the electronic and optical properties of XX or TX systems, Poisson–Schrödinger equation has been solved self-consistently by following the method in Ref. [39]. The XC potentials between same kind of particles have been calculated in the local density approximation which is improved by Perdew and Zunger [40]. Furthermore, in the determination of attractive and repulsive Coulomb terms, the effect of interface polarizations is taken into account during the calculations. Poisson equations for electrons and holes are

$$\nabla\kappa(r)\nabla\Phi_e=-q_e\rho_e(r) \quad (4)$$

$$\nabla\kappa(r)\nabla\Phi_h=-q_h\rho_h(r) \quad (5)$$

where $\kappa(r)$ is the dielectric constant of the material in which the electrons and holes move. $\rho_{e,h}(r)$ is the electron/hole density.

Oscillator strength, a unitless parameter, is very important quantity in an investigation of all optical properties of any quantum system. In a single exciton system, the oscillator

strength is called as [41]

$$f = \frac{E_p}{2E}\left|\int d^3 r \psi_e(r)\psi_h(r)\right|^2 \tag{6}$$

where E is transition energy, and E_p is the periodicity or in another word, Kane energy which includes the contribution of Bloch functions. If the number of excitons in a QD is more than one, the recombination oscillator strength is defined as [42]

$$f = A\frac{E_p}{2E}\left|\int d^3 r \psi_e(r)\psi_h(r)\right|^2 \tag{7}$$

where A represents the number of recombination possibilities in the excitonic system. For example, the A can be 2 or 4 for unbound XX or bound XX, respectively. Details of this approximation can be found in Refs. [39,42]

As can be seen from Figure 1, there are two possibilities for the recombination of electron–hole pairs in the TX. One of them is $1s-1s$ transition, and the other one is $1p-1p$ transitions. In $1s-1s$ transition, there are four recombination probabilities which are $e_1-h_1, e_2-h_2, e_1-h_2$ and e_2-h_1. For the sake of simplicity, we restricted ourselves to $1p-1p$ transition in the TX. In the case of electron–hole pair in p states, there is only one recombination probability and so we can use Equation (6) for the recombination oscillator strength of $1p-1p$ transition. It is noted that the effects of the s-state carriers on the energy levels and wave functions of p-state carriers are taken into consideration inherently due to the nature of self-consistent computation.

Furthermore, the lifetime for excitonic structures is

$$\tau = \frac{6\pi\varepsilon_0 m_0 c^3 \hbar^2}{e^2 n \beta_s E^2 f}, \tag{8}$$

where ε_0 is the dielectric permittivity of the vacuum, m_0 is the free electron mass, c is the light velocity in the vacuum, e is the electronic charge, f is the oscillator strength, n is the refractive index, E is the transition energy and β_s is the screening factor [43], which is given by

$$\beta_s = \frac{3\varepsilon}{\varepsilon_{QDNC} + 2\varepsilon}. \tag{9}$$

Here, ε and ε_{QDNC} correspond to the optical dielectric constants of the medium solvent and QDNC, respectively.

3. Results and discussion

In this study, the change in the optical and electronic properties of single exciton, biexciton and tri-exciton systems in CdSe/ZnS core–shell structure has been calculated by varying the core radius from 1.5 to 4.5 nm. In performed calculations, atomic units $\hbar = m_0 = e = 1$ are used.

The information about the energies of the states, the transition probabilities and their variation with QDNC's size are very important to understand the physics of excitonic

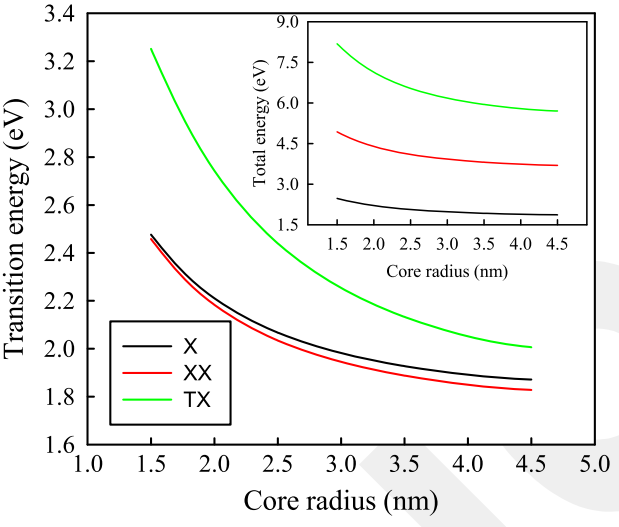

Figure 2. (colour online) The variation of the transition energies of single- (black), bi- (red) and tri- (green) excitons with increasing of the core radius. The inset shows the total energy changes of the each structure.

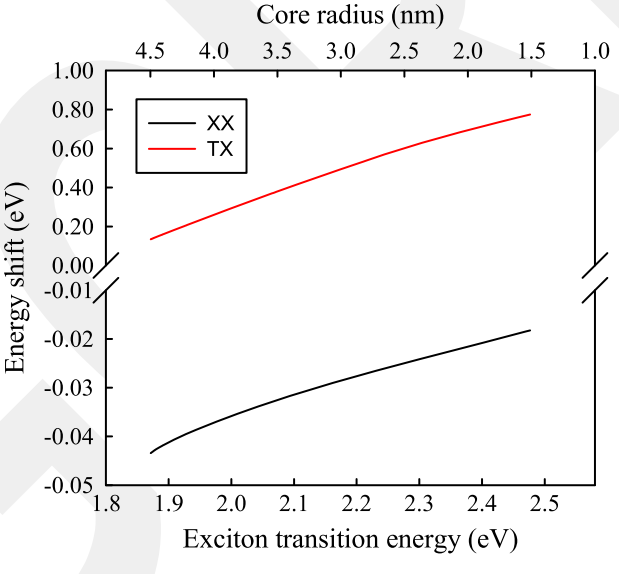

Figure 3. (colour online) The energy shifts changes of the biexction and triexciton as a function of the single exction transition energy and core radius.

structures. It is noted that we focus on just $p - p$ transition in the TX structure for the sake of simplicity by following some similar studies [29,35]. The effect of QDNC radius on the total and transition energies is shown in Figure 2. As is well known, in any quantum mechanical system, a diminishing dimension(s) lead(s) to an increase in energy of the system. This situation can be observed in Figure 2. As can be seen from this figure, for all the systems, both total and transition energies are decreasing with increasing of the core

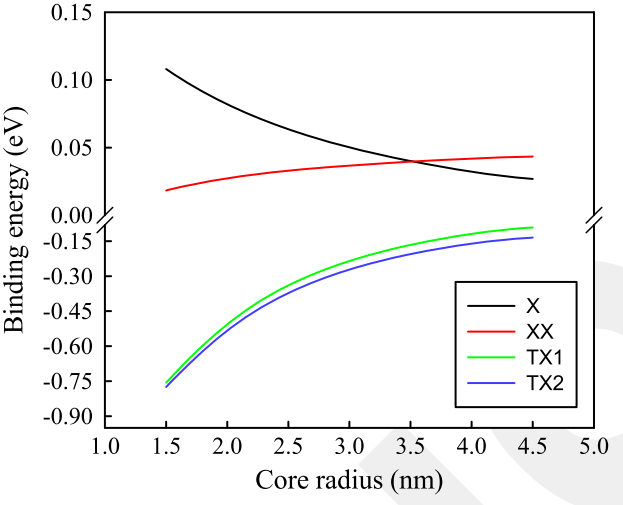

Figure 4. (colour online) The variation of binding energies with respect to the core radius for exciton (black curve) and biexciton (red curve) and triexciton (green and blue curves).

radius. This situation is a result of the quantum mechanics. In Figure 2, as can be seen in the inset, the total energies are separated dramatically from each other. On the other hand, the transition energy curves of the single X and XX structures are very close to each other especially for smaller core radii while the curve of the TX structure is remarkably higher than those of the single X and XX. The TX emission shows a blue-shift due to the recombination of the electron and hole in *p* state. Because of this, single- and bi-exciton systems can be experimentally distinguished from the triexciton structures while the single- and bi-exciton peaks are not easily distinguished from one another. These kinds of changes have been experimentally observed and reported by some authors [29].

An energy shift shows the amount of shift of the XX or TX peak energies according to single X peak energy and it can be determined by means of the transition energies. The difference between transition energies of the XX and single X gives the XX energy shift. Similarly, the difference between TX and single X transition energies will give the TX energy shift. Figure 3 shows the energy shifts of the XX and TX as a function of the single X transition energy and also core radius. As can be seen from Figure 3, the decrease in the size of the QDNC leads to an increase in the energy shift of both XX and TX structure with the single X transition energy. The possible reason of this situation is the dominant effect of repulsive Coulomb interaction between the identical carriers with decreasing core radius. Furthermore, the energy of the recombined electron–hole pairs in *p* states is higher than that of the pairs in the *s* ones. As can be seen from Figures 2 and 3, the tendency of the results are quite consistent with the experimental ones reported in the literature [28,29,44].

The binding energy is a useful tool for explanation of the repulsive and attractive interactions between carriers in the excitonic structures in a QDNC. In a XX structure, for example, if the binding energy is negative, it means that there are two independent excitons with small interaction with each other. The size of QDNC, exchange potentials between identical particles and number of charges have crucial effects on the variation of binding energy. Figure 4 shows the variation of the binding energy of the single X, XX and TX with increasing QDNC core radius. As can be seen from the figure, the exciton

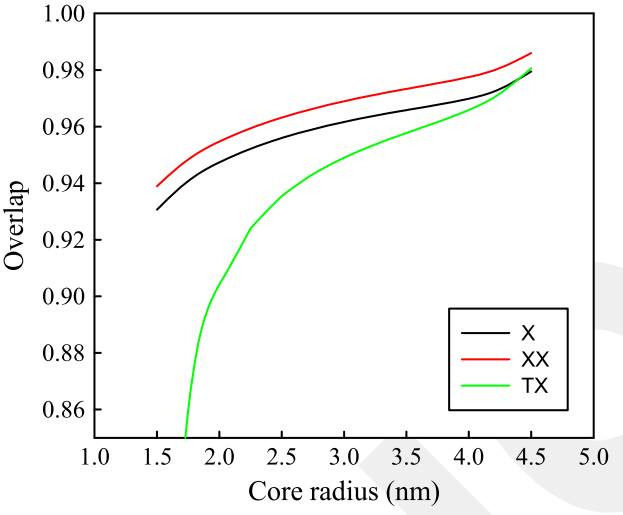

Figure 5. (colour online) The variation of the overlap integral of single exciton, biexciton and triexciton as a function of the core radius of the QDNC.

binding energy is decreasing with increasing of the core radius. For small core radius, the electron–hole pair is strongly confined in the same small spatial region which leads to a strong attractive Coulomb interaction and a strong binding energy between the carriers. On the other hand, when the core radius is increased, the confinement effect decreases and electron and hole behave like free particles and binding energy is rapidly decreasing. In the XX structure, for the case of small core radius, the binding energy is lower because of the repulsive interaction between the identical particles. The binding energy increases in the case of larger core radius because of the attractive interaction in the XX system. In the literature, there are two different formulas for the binding energy of the TX structure those are

$$TX_1 = 3E(X) - E(TX) \tag{10}$$

$$TX_2 = E(X) + E(XX) - E(TX). \tag{11}$$

In the TX system, a bound structure cannot be observed because of the high energy of the carriers and predominant repulsive Coulomb interactions between identical particles. In this system, the binding energy is very low in the case of small core radius and remarkably high in the case of large core radius. The main reason of this situation is the decrease in electron/hole energies and the domination of the attractive Coulomb interactions compared with repulsive ones depending on radius size. As seen from Figure 4, the curves of TX_1 and TX_2 are very similar, but the values of TX_2 are lower than those of TX_1. This case is the result of $3E(X) < (E(X) + E(XX))$. Furthermore, from Figure 4 one can see that the binding energy is increasing with the QDNC radius, which is the consequence of the decrease in repulsive interaction between identical particles with the increase in the core radius.

The overlap integral is also important parameter for the determination of optical properties such as oscillator strength and lifetime. Figure 5 shows the variation of overlap integral with respect to the quantum dot radius. When we look at the figure, we see that

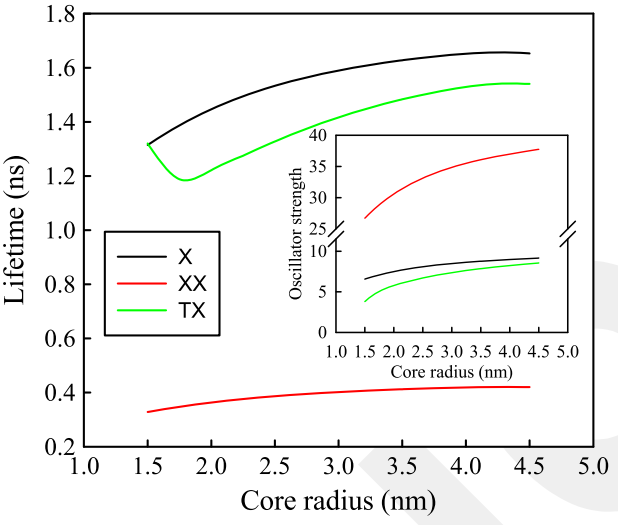

Figure 6. (colour online) The variation of lifetime of the single exciton, biexciton and triexciton depending on the increasing of QDNC core radius. The inset shows the oscillator strength of the each structure.

the overlap integrals of X and XX have almost same values and the changes of them with the core radius increase. These increases exhibit same tendency and approach to unity. The changes of the values of the overlap integral with the radius are between 0.94 and 0.98 for the single X and XX. This shows that the penetration of the wavefunctions of the electron(s) and hole(s) to the shell region is not too much and not dependent strongly on changes of the core radius from 1.5 to 4.5 nm. As regards the overlap integral of TX, its value starts from almost 0.7 and increases very rapidly with the core radius and approaches to the unity for the value of 4.5 nm of core radius as similar to the X and XX cases. The physical reason of these changes of the overlap integral of TX can be explained as follow: In small core radii, energy levels of 1*p* states both electron and hole is very high in comparison to 1*s* states and hence the penetration of the electron and hole wavefunctions of the *p* states to the shell region is also much more. As a result of this the overlap becomes smaller. The *p* energy levels decrease with increasing of the core radius and this leads to lower penetration to the shell region. Therefore, the overlap has larger values for large core radii.

The recombination lifetimes of excitonic structures can be crucial for device fabrications, such as photovoltaic, LED or laser applications, etc. Therefore, information about lifetime of any excitonic structure are so worthwhile. In addition, the lifetime can be measured directly and so it is important in view of the comparison of theoretical results with experimental ones. The recombination lifetime of the structure considered is calculated by using Equation (8). As seen from the equation, the transition energy and oscillator strength are effective on determination of the lifetime values. Figure 6 shows the changes in the lifetimes of the X, XX and TX as a function of the QDNC core radius. The inset demonstrates the changes in oscillator strength of the structures. The changes of lifetime values are not dramatic with the core radius of QDNC. The value of X lifetime lies between almost 1.3 and 1.6 ns. Similarly, the values of the TX changes between 1.2 and 1.5 ns. On the other hand, the lifetime of the XX is much shorter than those of the X and TX, and the

changes of values with the core radius are not remarkable. The physical reason of this can be explained as follow: Since the XX is a bound system, there are four different possibilities for the recombination of the carriers. In this case, as seen in the inset, the oscillator strength of biexciton is approximately four times bigger than other systems because of multiplication by 4 as explained details in Ref. [42].

4. Conclusions

Although there are experimental studies on multiexciton system and wide theoretical studies on the single exciton and biexciton structures, theoretical studies on the triexciton system in QDNCs have not been sufficiently introduced into the literature. With this work, we have intended to widely investigate the optical properties of the triexciton structure in quantum dot by comparing the results with that of single and biexciton systems. The properties such as absorption spectrum, radius dependent binding energy, transition energy, overlap integral, oscillator strength and lifetime have been calculated and compared with other single and biexciton systems. The results show that the triexciton exhibits different behaviours in comparison to single and biexciton behaviours. We believe that the results will be useful for further theoretical and experimental studies on the multiexction structures.

Funding

This work was supported by The Scientific and Technological Research Council of Turkey (TUBITAK) TBAG [project number 109T729].

References

[1] U.E.H. Laheld and G.T. Einevoll, *Excitons in CdSe quantum dots*, Phys. Rev. B 55 (1997), pp. 5184–5204.
[2] S. Rodt, R. Heitz, A. Schliwa, R.L. Sellin, F. Guffarth, and D. Bimberg, *Repulsive exciton-exciton interaction in quantum dots*, Phys. Rev. B 68 (2003), p. 035331.
[3] V. Mlinar and A. Zunger, *Internal electronic structure and fine structure of multiexcitons in semiconductor quantum dots*, Phys. Rev. B 80 (2009), p. 205311.
[4] M. Sahin, S. Nizamoglu, A.E. Kavruk, and H.V. Demir, *Self-consistent computation of electronic and optical properties of a single exciton in a spherical quantum dot via matrix diagonalization method*, J. Appl. Phys. 106 (2009), p. 043704.
[5] S. Brovelli, R.D. Schaller, S.A. Crooker, F. Garcia-Santamaria, Y. Chen, R. Viswanatha, J.A. Hollingsworth, H. Htoon, and V.I. Klimov, *Nano-engineered electron-hole exchange interaction controls exciton dynamics in core-shell semiconductor nanocrystals*, Nat. Commun. 2 (2001), p. 280.
[6] M. Sahin, S. Nizamoglu, O. Yerli, and H.V. Demir, *Reordering orbitals of semiconductor multi-shell quantum dot-quantum well heteronanocrystals*, J. Appl. Phys. 111 (2012), p. 023713.
[7] V.L. Colvin, M.C. Schlamp, and A.P. Alivisatos, *Light-emitting diodes made from cadmium selenide nanocrystals and a semiconducting polymer*, Nature 370 (1994), pp. 354–357.
[8] S. Coe, W.K. Woo, M. Bawendi, and V. Bulovic, *Electroluminescence from single monolayers of nanocrystals in molecular organic devices*, Nature 420 (2002), pp. 800–803.
[9] R.D. Schaller and V.I. Klimov, *High efficiency carrier multiplication in PbSe nanocrystals: Implications for solar energy conversion*, Phys. Rev. Lett. 92 (2004), p. 186601.
[10] D.J. Milliron, I. Gur, and A.P. Alivisatos, *Hybrid organic-nanocrystal solar cells*, MRS Bull. 30 (2005), pp. 41–44.

[11] V. Sundar, H.J. Eisler, T. Deng, Y. Chan, E.L. Thomas, and M.G. Bawendi, *Soft-lithographically embossed, multilayered distributed-feedback nanocrystal lasers*, Adv. Mater. 16 (2004), pp. 2137–2141.
[12] Y. Chan, J.-M. Caruge, P.T. Snee, and M.G. Bawendi, *Multiexcitonic two-state lasing in a CdSeCdSe nanocrystal laser,* Appl. Phys. Lett. 85 (2004), pp. 2460–2462.
[13] G. Burkard, D. Loss, and D.P. DiVincenzo, *Coupled quantum dots as quantum gates*, Phys. Rev. B 59 (1999), pp. 2070–2078.
[14] A. Imamoglu, D.D. Awschalom, G. Burkard, D.P. DiVincenzo, D. Loss, M. Sherwin, and A. Small, *Quantum information processing using quantum dot spins and cavity QED*, Phys. Rev. Lett. 83 (1999), pp. 4204–4207.
[15] T. Fujisawa, T. Hayashi, and S. Sasaki, *Time-dependent single-electron transport through quantum dots*, Rep. Prog. Phys. 69 (2006), pp. 759–796.
[16] W.M. Witzel, X. Hu, and S.D. Sarma, *Decoherence induced by anisotropic hyperfine interaction in Si spin qubits*, Phys. Rev. B 76 (2007), p. 035212.
[17] F. Baruffa, P. Stano, and J. Fabian, *Theory of anisotropic exchange in laterally coupled quantum dots,*Phys. Rev. Lett. 104 (2010), p. 126401.
[18] S. Pathak, E. Cao, M.C. Davidson, S. Jin, and G.A. Silva, *Quantum dot applications to neuroscience: New tools for probing neurons and glia*, J. Neurosci 26 (2006), pp. 1893–1895.
[19] Y. Liu, R. Brandon, M. Cate, X. Peng, R. Stony, and M. Johnson, *Detection of pathogens using luminescent CdSe/ZnS dendron nanocrystals and a porous membrane immunofilter,* Anal. Chem. 79 (2007), pp. 8796–8802.
[20] S. Hennig, S. van de Linde, M. Heilemann, and M. Sauer, *Quantum dot triexciton imaging with three-dimensional subdiffraction resolution*, Nano. Lett. 9 (2009), pp. 2466–2470.
[21] M. Heidbreder, U. Endesfelder, S. van de Linde, S. Hennig, D. Widera, B. Kaltschmidt, C. Kaltschmidt, and M. Heilemann, *Subdiffraction fluorescence imaging of biomolecular structure and distributions with quantum dots*, Biochim. Biophys. Acta 1803 (2010), pp. 1224–1229.
[22] J.H. Werner, S. Kolodinski, and H.J. Queisser, *Novel optimization principles and efficiency limits for semiconductor solar cells,* Phys Rev. Lett. 72 (1994), pp. 3851–3854.
[23] C. Smith and D. Binks, *Multiple exciton generation in colloidal nanocrystals,* Nanomaterials 4 (2014), pp. 19–45.
[24] G. Zohar, R. Baer, and E. Rabani, *Multiexciton generation in IV-VI nanocrystals: The role of carrier effective mass, band mixing, and phonon emission,* J. Phys. Chem. Lett. 4 (2013), pp. 317–322.
[25] V.I. Klimov, *Spectral and dynamical properties of multiexcitons in semiconductor nanocrystals,* Annu. Rev. Phys. Chem. 58 (2007), pp. 635–673.
[26] A.J. Nozik, *Multiple exciton generation in semiconductor quantum dots*, Chem. Phys. Lett. 457 (2008), pp. 3–11.
[27] M. Ikezawa, Y. Masumoto, T. Takagahara, and S.V. Nair, *Biexciton and triexciton states in quantum dots in the weak confinement regime*, Phys. Rev. Lett. 79 (1997), pp. 3522–3525.
[28] J.-M. Caruge, Y. Chan, V. Sundar, H.J. Eisler, and M.G. Bawendi, *Transient photoluminescence and simultaneous amplified spontaneous emission from multiexciton states in CdSe quantum dots*, Phys. Rev. B 70 (2004), p. 085316.
[29] D. Oron, M. Kazes, I. Shweky, and U. Banin, *Multiexciton spectroscopy of semiconductor nanocrystals under quasi-continuous-wave optical pumping,* Phys. Rev. B 74 (2006), pp. 115333.
[30] B. Fisher, J.M. Caruge, D. Zehnder, and M. Bawendi, *Room-temperature ordered photon emission from multiexciton states in Single CdSe Core-Shell Nanocrystals,* Phys. Lett. 94 (2005), p. 087403.
[31] A. Barenco and M.A. Dupertuis, *Quantum many-body states of excitons in a small quantum dot*, Phys. Rev. B 52 (1995), pp. 2766–2778.
[32] A. Wojs and P. Hawrylak, *Exciton-exciton interactions in highly excited quantum dots in a magnetic field*, Solid State Commun. 100 (1996), pp. 487–491.
[33] S. Raymond, P. Hawrylak, C. Gould, S. Fafard, A. Sachrajda, M. Potemski, A. Wojs, S. Charbonneau, D. Leonard, P.M. Petroff, and J.L. Merz, *Exciton droplets in zero dimensional systems in a magnetic field,* Solid State Commun. 101 (1997), pp. 883–887.

[34] P. Hawrylak, *Excitonic artificial atoms: Engineering optical properties of quantum dots*, Phys. Rev. B 60 (2001), pp. 5597–5608.
[35] A. Franceschetti and M.C. Troparevsky, *Radiative recombination of triexcitons in CdSe colloidal quantum dots*, J. Phys. Chem. C 111 (2007), pp. 6154–6157.
[36] R.B. Little, M.A. El-Sayed, G.W. Bryant, and S. Burke, *Formation of quantum-dot quantum-well heteronanostructures with large lattice mismatch: ZnS/CdS/ZnS*, J. Chem. Phys. 114 (2001), pp. 1813–1822.
[37] S.A. Ivanov, J. Nanda, A. Piryatinski, M. Achermann, L.P. Balet, I.V. Bezel, P.O. Anikeeva, S. Tretiak, and V.I. Klimov, *Light amplification using inverted core/shell nanocrystals: towards lasing in the single-exciton regime*, J. Phys. Chem. B 108 (2004), pp. 10625–10630.
[38] D. Battaglia, J.J. Li, Y. Wang, and X. Peng, *You have full text access to this contentColloidal two-dimensional systems: CdSe quantum shells and wells,* Angew. Chem., Int. Ed. 42 (2003), pp. 5035–5039.
[39] A. Akturk, M. Sahin, F. Koc, and A. Erdinc, *A detailed investigation of electronic and optical properties of the exciton, the biexciton and charged excitons in a multi-shell quantum dot nanocrystal*, J. Phys. D: Appl. Phys. 47 (2014), pp. 285301.
[40] J.P. Perdew and Alex Zunger, *Self-interaction correction to density-functional approximations for many-electron systems,* Phys. Rev. B 23 (1981), pp. 5048–5079.
[41] J.H. Davies, *The Physics of Low-Dimensional Semiconductors: An Introduction*, Cambridge University Press, Cambridge, England, 1996.
[42] M. Sahin and F. Koc, *A model for the recombination and radiative lifetime of trions and biexcitons in spherically shaped semiconductor nanocrystals,* Appl. Phys. Lett. 102 (2013), p. 183103.
[43] B. Alen, J. Bosch, D. Granados, J. Martinez-Pastor, J.M. Garcia, and L. Gonzalez, *Oscillator strength reduction induced by external electric fields in self-assembled quantum dots and rings,* Phys. Rev. B 75 (2007), p. 045319.
[44] C. Bonati, M.B. Mohamed, D. Tonti, G. Zgrablic, S. Haacke, F. van Mourik, and M. Chergui, *Spectral and dynamical characterization of multiexcitons in colloidal CdSe semiconductor quantum dots,* Phys. Rev. B 71 (2005), p. 205317.